

# Structural changes in DODAC unilamellar liposomes by addition of sucrose esters monitored by using fluorescent techniques

E. Lemp, A.L. Zanocco, G. Günther\*

*Departamento de Química Orgánica y Fisicoquímica, Facultad de Ciencias Químicas y Farmacéuticas,  
Universidad de Chile, Casilla 233, Santiago 1, Chile*

---

## Abstract

The effect of the incorporation of the non-ionic surfactant sucrose palmitate in dioctadecyldimethylammonium chloride (DODAC) large unilamellar vesicles was studied by using several spectroscopic techniques. Significant changes in the liposome bilayer were detected prior to the formation of mixed micelles. Turbidity experiments show major growth in vesicle size. This behavior is rarely observed in large unilamellar vesicles. The vesicle size increase is accompanied by several alterations of the lipidic bilayer. Fluorescence of 6-dodecanoyl-2-(dimethylamino)-naphthalene (Laurdan) and pyrene incorporated in liposomes shows a dependence on sucrose palmitate addition, this is compatible with modifications of polarity and fluidity of its surroundings, probably due to a decrease in the bilayer water content. In contrast, diphenylhexatriene anisotropy changes indicate that deeper microenvironments are not substantially affected. In addition, changes in the quenching constant of pyrene and its derivatives by oxygen are indicative of the increase in oxygen solubility when the sucrose ester is incorporated in the liposome. These changes in the structure-dependent properties of DODAC liposome bilayer are explained by the location of the voluminous co-surfactant sucrose head groups on the liposome surface.

*Keywords:* Liposomes solubilization; Palmitoyl sucrose; Pyrene; Pyrene derivatives; Laurdan

---

## 1. Introduction

Solubilization and reconstitution of biological membranes by using surfactants has captured the attention of biochemists and chemists since the mid-1970s [1–7]. In these studies, involving several surfactant–liposome systems, the interaction between surfactant and liposome structure has been always described in terms of a three-stage model [4]. In the first stage (stage I), the surfactant is distributed between liposome and the aqueous phase. In stage II,

upon liposome bilayer saturation, the mixed liposome evolves into mixed micelles. The last stage (stage III), corresponds to a decrease of lipid/surfactant ratio in previously formed mixed micelles. We are particularly interested in the study of changes promoted by the incorporation of the non-ionic surfactant sucrose palmitate into the liposome at stage I. The ability of surfactants to induce both changes in the water–liposome interface and in the lipidic bilayer structure is crucial in order to understand the nature of the interactions between physiologically active molecules and liposome bilayers. Of particular interest is this knowledge in the design and optimization

---

\* Corresponding author.

of newer technological applications [8,9]. Nowadays, non-ionic surfactants are being widely employed, because they are readily incorporated as co-surfactants into liposomes [4,8,10] or as alternatives to ionic surfactants, forming microaggregates (niosomes) [11–14]. Non-ionic surfactants generally are cheap and successful alternatives of non-biological origin. A particularly interesting group of surfactants that can be employed as co-detergents to form mixed liposomes are the fatty acid esters of monosaccharides and disaccharides. These kinds of surfactants have unique properties being non-toxic, skin compatible, non-polluting and biodegradable. Also, their obtainment is not dependent on the petrochemical industry and they can be made from renewable sources. However, due to the difficulties to synthesize and purify sucrose monoesters [15,16], only a limited number of experimental studies that concern their physico-chemical properties have been carried out with pure compounds [17]. Currently, mixtures of mono and polyesters, or mixtures of several monoesters are being used. A classical example is the use of the WASAG<sup>®</sup> series, mixtures in which hydrophobicity is controlled by varying the length of the alkyl chains and the proportion of mono- and polyesters [18].

In this work, we studied the effect of the incorporation of a unique isomer of sucrose monopalmitate, PAL, on the structure and the physico-chemical properties of dioctadecyldimethylammonium chloride (DODAC) liposomes. Several fluorescent probes were selected to sense specific properties of both the more hydrophobic regions of the liposome bilayer and the water–liposome interface, to gain a better understanding of the effect of surfactant incorporation.

An amphiphilic fluorophore, such as 6-dodecanoyl-2-(dimethylamino)-naphthalene (Laurdan), incorporates into membranes with the fluorescent moiety localized in the region of the acyl bonds on the glycerol backbone of phospholipids [19]. Therefore, spectroscopic behavior of this probe in the microaggregate is related to the membrane polarity and/or the membrane fluidity (gel or fluid lamellar phase) [20], because of its sensitivity to the solvent dielectric relaxation effects. Also, according to recent data, measurements of Laurdan fluorescence polarization can be used to monitor perturbations of membrane ordering [21]. Lipid packing below the lipid phase transition temperature restricts the movements of associated

water molecules and above this freedom of dipolar motion increases. These differences are reflected in emission spectra of Laurdan [22], allowing its use as a valuable probe in observing physico-chemical micro-properties in compartmentalized systems. To account for observed emission shifting in Laurdan spectra, a well-known parameter is the change in generalized polarization (GP). High values of GP are ascribed to a less fluid surrounding [23].

Another hydrophobic fluorescent membrane probe, 1,6-diphenylhexatriene (DPH), is slightly sensitive to environment polarity, and it is primarily used to estimate the internal viscosity of the bilayers by measuring fluorescence polarization or anisotropy. In addition, pyrene is a very useful fluorescent probe due to the sensitivity of its fluorescence spectra and singlet state lifetime to the properties of the environment where it is solubilized. Also, the excited pyrene–oxygen interaction rate is indicative of oxygen accessibility to the probe location. Considering the relatively free pyrene motion, several carboxylic derivatives of this aromatic compound, with different alkyl chains and a carboxylic acid terminal, are adequate to anchor the probe at different bilayer depths.

## 2. Experimental

### 2.1. Chemicals

Sucrose palmityl ester ( $\beta$ -D-fructofuranosyl-6-O-palmityl- $\alpha$ -D-glucopyranoside (PAL)) was synthesized by the Lindhart et al.'s procedure [24] that yields a relatively complex mixture of monoesters (mainly 6-O and presumably 3-O), di- and triesters. Preparative HPLC was employed to isolate PAL. DODAC from Herga Ind. (Brazil) was purified as described elsewhere [25]. Pyrene and DPH from Sigma and pyrene decanoic acid (PyC10) and Laurdan from Molecular Probes were used as received.

### 2.2. Isolation and characterization of palmityl sucrose

Semipreparative low-pressure liquid chromatography was performed by using a LOBAR LiChroprep<sup>®</sup> RP-18 (40–63  $\mu$ m) column (Merck) attached to a Shimadzu LC-9A HPLC pump. Methanol–water (70:30)

at 2.00 ml/min was the mobile phase. The composition of collected fractions was observed by using thin layer chromatography employing chloroform–methanol (4:1) to elute samples and staining with a butanolic solution of urea–orthophosphoric acid. The purity of isolated PAL, after combining the fractions containing the ester, removing the solvent and drying in vacuo, was monitored in a Waters 600 HPLC system, equipped with a Waters PDA detector (at 205 nm) and a Merck LiChrospher® 60 RP Select B (5  $\mu$ m) column. Experiments were carried out in the isocratic mode by employing methanol–water (70:30) at 1.00 ml/min, as the mobile phase. The NMR spectra of PAL, performed in a Bruker ADX 300 spectrometer in DMSO<sub>d-6</sub> containing 5% of CH<sub>3</sub>OD, to avoid micellization, agrees well with the previously reported spectra [24].

### 2.3. Liposome preparation

Large unilamellar liposomes (LUVs) were obtained by controlled injection of a DODAC–chloroform solution (20 mM) in Milli-Q water thermostated at  $75 \pm 0.5$  °C, according to the procedure previously described [25]. The final concentration was fixed by the amount of DODAC–chloroform solution injected.

### 2.4. Fluorescence spectroscopy

Steady state fluorescence measurements of pyrene and Laurdan were accomplished in a Fluorolog Tau-2 spectrofluorometer (SPEX, Jobin Ybon). Anisotropy and polarization measurements of DPH (2.5  $\mu$ M,  $\lambda_{\text{ex}} = 350$  nm,  $\lambda_{\text{em}} = 450$  nm) were carried out in a LS-50B (Perkin-Elmer) spectrofluorimeter. Time-resolved fluorescence lifetimes of pyrene and pyrene derivatives ( $5.0 \times 10^{-6}$  M), gave no spectral evidence of excimer formation,  $\lambda_{\text{ex}} = 337$  nm. The oxygen quenching constants were measured in a custom-made system that is comprised of a nitrogen laser PL 2300 (PTI), a custom-wired photomultiplier R928 (Hamamatsu) connected to an oscilloscope TDS 3032 (Tektronix). Data were acquired and processed with a language G Labview based software. All the above-mentioned equipment and systems were temperature controlled within 0.5 °C.

### 2.5. Turbidity

UV-Vis dispersion determinations were carried out on an UV-4 spectrophotometer (Unicam). Dispersion was also observed in fluorescence experiments carried out on Fluorolog Tau-2 spectrofluorimeter (SPEX, Jobin Ybon).

## 3. Results and discussion

### 3.1. Effect of palmityl sucrose addition on liposome properties

The influence of sucrose ester addition on the properties and stability of DODAC liposomes was studied using different fluorescent probes and several experimental techniques.

Solubility of PAL in water was assessed by measuring fluorescence intensity and generalized polarization of Laurdan at 425 nm. Fig. 1 shows the dependence of both parameters as a function of PAL concentration. Fig. 1 shows that the Laurdan fluorescence intensity at 425 nm increases linearly at low PAL concentration whereas the GP values decreases linearly in the same PAL concentration range. Both parameters display a sharp break point at PAL concentration of  $(1.97 \pm 0.16) \times 10^{-5}$  M. Above this PAL concentration, the GP values remain practically unchanged and the fluorescence intensity of Laurdan increases very slowly. These changes in spectroscopic behavior of Laurdan can be ascribed to surfactant micellization, which yields a critical micellar concentration (cmc) of  $(1.97 \pm 0.16) \times 10^{-5}$  M for PAL. This cmc value agrees with literature reported values equal to  $1.74 \times 10^{-5}$  and  $1.81 \times 10^{-5}$  M [24]. This result implies that the solubility of PAL in water is very low and indicates that it will incorporate into DODAC liposomes with a very low concentration as free ‘detergent’ in the aqueous pseudophase.

To study the effect of PAL addition on the structure and physico-chemical properties of DODAC liposomes in stage I, it was necessary to determine the range of PAL concentrations at which DODAC liposomes remain intact. The transformation of liposomes (lamellar structures) into mixed micelles, sometimes termed ‘solubilization’, takes place when the ratio of concentrations of detergent to lipid ( $R$ , present in the

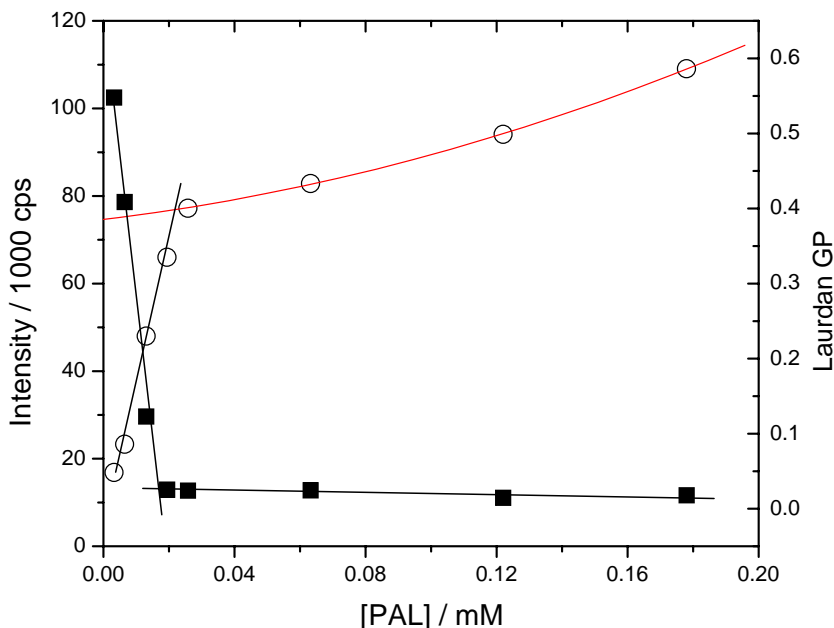


Fig. 1. Changes of Laurdan emission intensity ((○) 425 nm and (■) Laurdan GP) as a function of PAL concentration. Both properties show a break point upon micellization at  $[PAL] = (1.97 \pm 0.16) \times 10^{-5}$  M, corresponding to the cmc at 20.0 °C ( $\lambda_{ex} = 365$  nm).

bilayer) reaches a critical value, represented as  $R_c$  [26]. This condition is achieved when the aqueous concentration of detergent in aqueous pseudophase equals its cmc [26]. To examine the effect of increasing PAL concentration on DODAC liposome structure and to monitor mixed micelle formation, we employed turbidity measurements. Fig. 2 shows the changes of dispersion at 400 nm of DODAC liposome solutions at different DODAC concentrations. Scattered light increases considerably and monotonically and, upon PAL addition, independent of liposome concentration. All plots show that scattered light has an abrupt break point when the sucrose ester concentration is twice than that of DODAC, giving an  $R_c$  value near 2.

Similar results were found from our steady-state fluorescence polarization study of the effect of PAL upon DPH-labeled DODAC liposomes. The anisotropy dependence of DPH on PAL incorporation into liposomes is depicted in Fig. 3. At  $R$  values below 0.75, DPH anisotropy is insensitive to PAL presence, whereas for  $R$  in the range between 1 and 2, DPH anisotropy decreases from 0.255 to 0.185. This latter value indicates DPH anisotropy is measured in a DODAC–PAL mixed micelle environment.

To evaluate the dependence of the micropolarity of DODAC liposomes on PAL incorporation to the bilayer, we used pyrene as a fluorescent probe. It is well known that the vibrational structure of the pyrene fluorescence spectrum and the ratio between emission bands I and III (ratio I/III) are very sensitive to micropolarity of the environment where pyrene is located [27,28]. Ratio I/III could also be convenient to monitor changes due to liposome solubilization. Fig. 4 shows the progression of ratio I/III when PAL is incorporated in DODAC liposomes. Data in Fig. 4 show a clear decrease of ratio I/III when PAL incorporates in the liposome, independent of liposomes concentration. This result is compatible with a decrease of micropolarity of the environment sensed by the probe. It has been reported that when pyrene is employed in high proportion (10 mol%), liposomes undergo shape transitions and/or size changes by an increase of membrane area due to enhanced space requirement of photoexcited probe [29]. In our experiments using pyrene, this effect can be disregarded because of the low pyrene concentration employed. In addition, turbidity measurements did not show any evidence of changes in the DODAC liposome

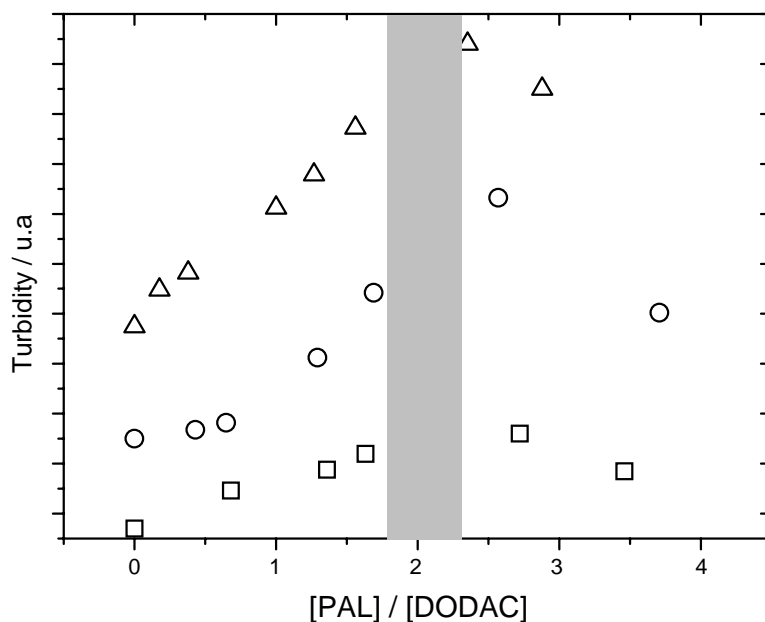


Fig. 2. Turbidity (400 nm) of aqueous solutions of DODAC liposomes as a function of PAL addition. [DODAC]: ( $\square$ ) 1 mM; ( $\circ$ ) 2 mM; ( $\Delta$ ) 4 mM. All cases shows a significant increase of dispersed light on PAL incorporation into the liposome. This result can be attributed to a increase in the vesicle size. Also there is a break point, the beginning of liposome ‘solubilization’, when [PAL]/[DODAC] takes a value near 2.0.  $T = 20 \pm 0.5^\circ\text{C}$ .

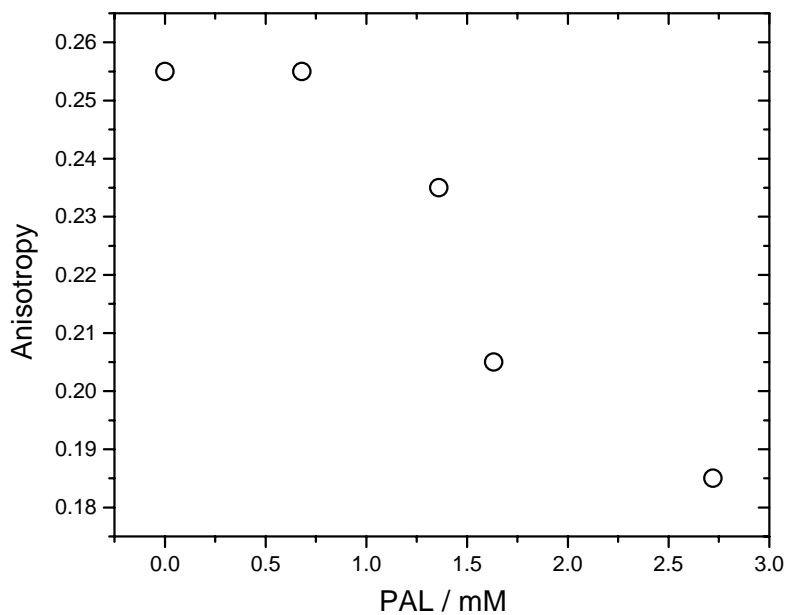


Fig. 3. Progression of DPH anisotropy ( $\lambda_{\text{ex}} = 350 \text{ nm}$ ,  $\lambda_{\text{em}} = 450 \text{ nm}$ ) as function of  $R$  measured in 1 mM DODAC liposomes. No dependence is observed until solubilization begins, at  $R$  over 1.0.  $T = 20 \pm 0.5^\circ\text{C}$ .

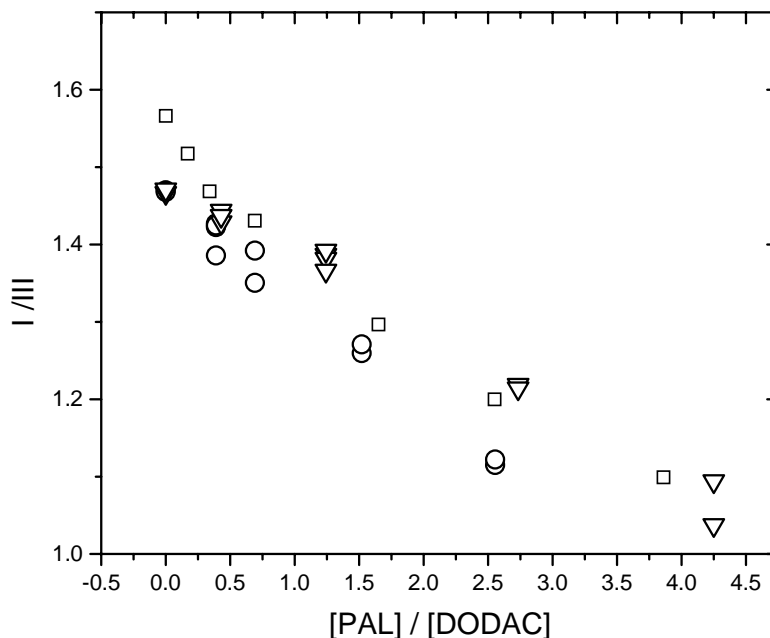


Fig. 4. Dependence of the ratio between bands I (371 nm) and III (382 nm) of pyrene fluorescence ( $\lambda_{\text{ex}} = 350$  nm),  $I_{\text{I}}/I_{\text{III}}$ , on the incorporation of PAL to DODAC liposomes at several concentrations of DODAC. A decrease of micropolarity sensed by the probe, independent on DODAC concentration, was observed. [DODAC]: ( $\square$ ) 0.5 mM, ( $\circ$ ) 1 mM; ( $\nabla$ ) 2 mM.  $T = 20 \pm 0.5^\circ\text{C}$ .

structure caused by pyrene incorporation to the membrane.

In order to obtain further information related to changes in physico-chemical properties of the liposome bilayer such as fluidity and/or polarity upon PAL addition, we carried out Laurdan generalized polarization measurements. Fig. 5 shows that GP is strongly dependent on  $R$ , although independent of DODAC concentration. For low values of  $R$ , the GP value increases from  $-0.30$  ( $R = 0$ ) to  $0.40$  ( $R = 1.75$ ). For  $R$  ranging between 1.75 and 2.0, GP begins to decrease, indicating a loosely packed microenvironment, ascribed to mixed micelle formation (liposome solubilization). The lowest expected value for GP should be 0.02, a value determined for Laurdan-labeled PAL micelles. As mentioned earlier, turbidity experiments show for  $R_e$  a value near 2.0, slightly larger than that measured with Laurdan.

According to Lichtenberg [6],  $R_e$  can be related to the partition constant  $K$ , and the cmc of the surfactant. From the  $R_e$  values between 1.0 and 2.0, measured by dispersion and fluorescence experiments and using a modification of the Lichtenberg [6] proposi-

tion (Eq. (1)), a  $K_\chi$  value for PAL partition between DODAC liposomes and the aqueous phase about of  $2 \times 10^6$ , was obtained. This value implies that essentially all the sucrose ester incorporates into the bilayer.

$$R_e = \left\{ \frac{55.5}{K_\chi \text{ cmc}} - 1 \right\}^{-1} \quad (1)$$

In previous studies of the solubilization process in phosphatidylcholine (DPPC) [5] and phosphatidylcholine/phosphatidic acid (EPC/EPA) liposomes [3,20], induced by octyl glucoside (OG, cmc = 22 mM), sodium dodecyl sulfate (SDS, cmc = 8.00 mM) or Triton X-100 (cmc = 0.15 mM), it was reported that dispersion increases slightly before bilayer solubilization. Also, it was shown that when the solubilization process begins, there is an important reduction in the intensity of scattered light. In a recent study of the solubilization process of giant vesicles, involving a wide number of lipids and detergents [7], different behaviors were observed, where the most common were a stepwise or smooth shrinkage. For non-ionic surfactants such as OG,  $R_e$  takes values

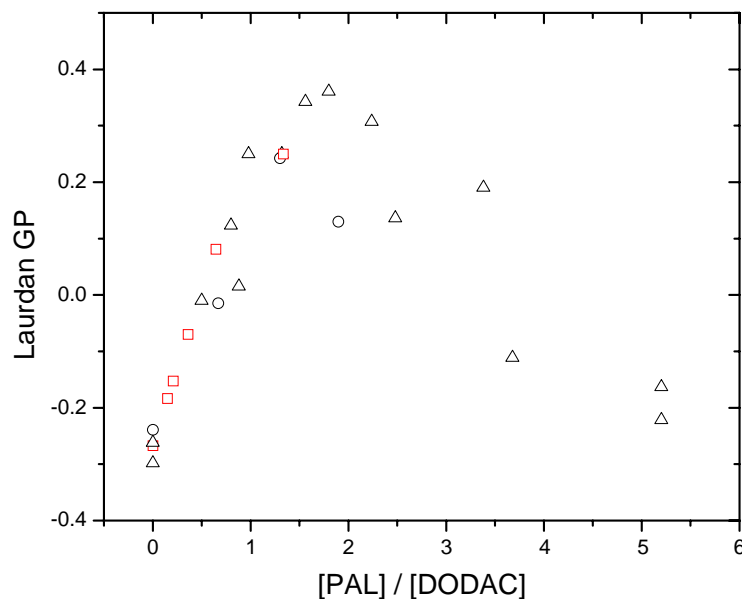


Fig. 5. Changes of Laurdan GP during addition of PAL in LAURDAN-labeled liposomes at 20 °C. When the [PAL]/[DODAC] ratio reaches a value of 1.0, there is a slope change indicating the beginning of major changes in the probe microenvironments. The behavior is not function of DODAC concentration, almost before solubilization. [DODAC]: ( $\Delta$ ) 0.5 mM; ( $\circ$ ) 1 mM; ( $\square$ ) 2 mM.

over 10.0 [5,20], for Triton X-100 near 1.0, and for ionic surfactants like SDS,  $R_e$  is near 1.0 or 2.0.

Our results indicate that the DODAC–PAL system in stage I of the solubilization process behave in a dissimilar manner to those previously studied. The large increase of scattered light at low PAL concentration can be explained in terms of an enlargement of the liposome upon incorporation of PAL in the bilayer. In a previous work [26], an increase of turbidity at the beginning of the solubilization process has been observed for small unilamellar vesicles (SUVs), however, also at this stage LUVs usually do not show turbidity changes, and solubilization is accompanied by turbidity diminution [26]. These differences could be related to the structural characteristics of PAL, mainly the large number of hydroxylic groups in the polar head. The observed decrease of the intensity of scattered light, when  $R$  is near 2.0, is compatible with formation of the first mixed micelles with simultaneous reduction in the liposome size as has been described previously [26].

Comparison of DPH anisotropy and turbidity measurements indicates that addition of low PAL concentration  $R < 1$ , produces significant structural changes

at the water–liposome bilayer interface whereas the inner core, which is sensed by DPH remains unaltered. In addition,  $R_e$  values determined from DPH anisotropy measurements are smaller than those obtained from turbidity experiments. The observed differences can be explained in terms of induced micellization or pre-micellization on the liposome surface, so that the solubilization conditions are reached concomitant with anisotropy reduction, but the system seems to be larger, as indicated by light dispersion.

The pyrene ratio I/III is not adequate for monitoring the liposome solubilization process. The observed value of the ratio I/III of pyrene emission in neat liposomes (1.6) is lower than that observed in water (1.8) and similar to that in acetone or ethylene glycol [30], indicating that pyrene is located near to the water–liposomes bilayer interface. No discontinuity was observed upon ‘solubilization’, in the range of  $R$  values employed. However, its decrease indicates that PAL addition could impede the access of water molecules to the site where the probe is localized and/or impel to pyrene move deeper into the liposome bilayer. The values of ratio I/III at higher  $R$ , between 1.05 and 1.1, could be indicative of mixed micelle



formation. A similar ratio I/III of 1.07 was determined for 0.2 mM PAL micelle solutions at 20 °C. Values of 1.06, 1.16 and 1.12 have been reported for SDS, Brij-35 and CTAC micelles, respectively [31].

On the other hand, changes observed on GP at low  $R$  values, could be related to two possible effects. The probe is sensing a more gelified environment, in which the lipidic packing would restrict the motion of dielectrically associated molecules. This makes dielectric relaxation less probable (the emission band centered near 435 nm is higher) and/or micropolarity of the Laurdan environment diminishes as a result of hindrance to water penetration (by presence of sucrose moieties on the liposome surface). The hypsochromic shift upon PAL addition, explained in terms of micropolarity decrease near to the probe, can be ascribed to a diminution in water content inside the liposome bilayer. The PAL incorporation could produce several effects on the bilayer structure of DODAC liposomes. The bulky sucrose head groups of PAL could modify the charge density on the liposome surface and sterically block channels for water penetration. In addition, insertion of a non-charged PAL between a pair of DODAC molecules can diminish, at least partially the head to head repulsion of DODAC in the water–liposome interphase. Additionally, hydrogen bond interactions between hydroxylic groups of sucrose could further contribute to blocking water access. Moreover, decrease in membrane fluidity can be due to the minor water content inside the liposome, concomitant with an increase of chain–chain hydrophobic interactions which results in a less-fluid bilayer. For the same  $R$  value, our results show that PAL addition does not modify anisotropy of DPH incorporated into a liposome. These results, apparently contradictory, could be understood if DPH and Laurdan are sensing different microenvironments in the liposome bilayer. A more hydrophobic probe such as DPH would be located deeper in the bilayer sensing a micromedia which water molecules cannot access, then, PAL addition does not produce significant structural modifications at low PAL content in this zone. Considering that the PAL and DODAC hydrocarbon chains are practically the same, no microviscosity changes deep in the bilayer should follow at low PAL incorporation in the liposome. Addition of PAL produces different effects on the surface and the inner bilayer of DODAC liposomes.

It is interesting to consider the differences of Laurdan emission spectra when it is incorporated into DPPC, EPC/EPA or DODAC liposomes. The emission spectra obtained in DPPC microaggregates, below the transition temperature shows only the lower wavelength band (434 nm), meaning a very restrictive gel lamellar phase [20], whereas in the EPC/EPA and DODAC, an additional shoulder appear at the red edge in the emission spectra indicating a less gelified microenvironment near to the probe. The effect of OG addition to EPC/EPA liposomes before the beginning of ‘solubilization’, unlike that observed for PAL addition to DODAC liposomes, leads to intensity decrease of the blue band compared with the red one and a red shift of the whole spectra. The differences in the spectroscopic behavior of Laurdan, reported for OG and those obtained for PAL, can be explained in terms of dissimilar modifications of the membrane surface [32] due to volume differences between glucose and sucrose polar head groups of OG and PAL, respectively. More significant changes in the surface charge density would be expected with PAL addition, as a consequence of the liposome size increase and due to the larger number of OH groups in the sucrose moiety that could interact by hydrogen bonds.

### *3.2. Effect of PAL addition on the phase transition temperature of DODAC liposomes*

In addition to the above-described studies, we examined the effect of PAL addition on the phase transition temperature of DODAC LUVs, employing DPH anisotropy measurements. Fig. 6 shows the dependence of DPH anisotropy with temperature for DODAC and DODAC/PAL ( $R = 0.5$ ) vesicles. DPH anisotropy observed in DODAC LUVs, shows an important decrease in the 30–50 °C range. Furthermore, near the phase transition temperature DPH anisotropy exhibit anomalous changes and the curve shows two up and down peaks that depart from the regular behavior. The same effect has been reported by Lissi et al. [33] observing temperature effects on both, ratios I/III and pyrene lifetimes incorporated into DODAC and DPPC LUVs. This anomalous behavior was ascribed to a particularly higher water penetration in the DODAC bilayer at the phase transition temperature, increasing ratio I/III values and decreasing pyrene lifetimes. Anomalies in the vicinity of the phase transition



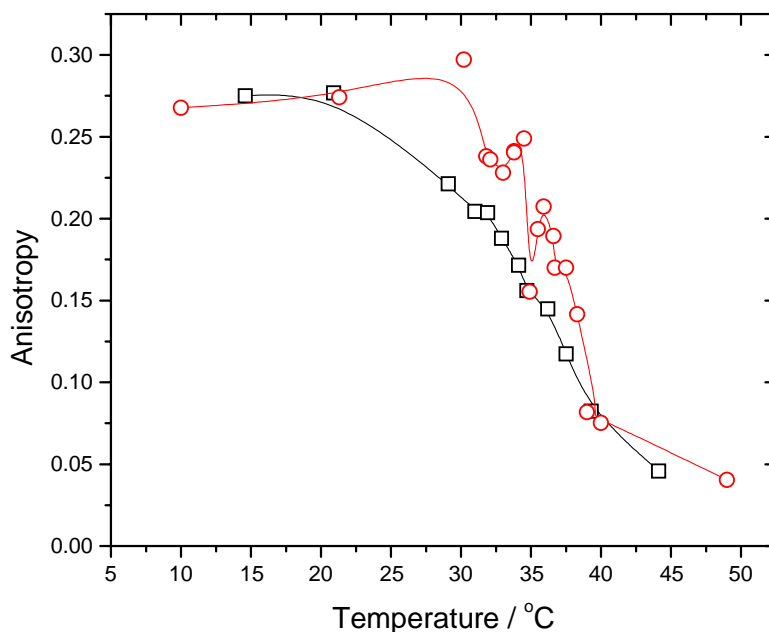


Fig. 6. Anisotropy of DPH ( $\lambda_{\text{ex}} = 350 \text{ nm}$ ,  $\lambda_{\text{em}} = 450 \text{ nm}$ ) in DODAC (○) and PAL/DODAC (□) vesicles as a function of temperature. [DODAC] = 1 mM;  $R = 0.4$ .

temperatures were not found when PAL was added to a DODAC liposome ( $R = 0.5$ ), as shown in Fig. 6. When PAL is incorporated, the anisotropy of DPH diminishes regularly from about 0.25 at 25 °C to 0.05 at 45 °C. The different behavior of the dependence of DPH anisotropy on the temperature in net DODAC and DODAC–PAL liposomes further supports our proposition that PAL addition to DODAC vesicles restricts water penetration inside the bilayer due to the sucrose moiety present at the interface. PAL incorporation only leads to minor differences at the phase transition temperatures since in this temperature range only slightly lower microviscosities are sensed by the fluorescent probe DPH. The same effect of PAL addition on phase transition temperatures was sensed by employing the Laurdan GP. Fig. 7 shows that in DODAC liposomes Laurdan generalized polarization decreases regularly when temperature increases from 15 to 32.5 °C. A major slope change is observed at the phase transition temperature zone and a small decrease in GP value is observed above this point. PAL incorporation into the bilayer increases GP, but an effect on the phase transition temperature was not observed although the range for transition seems to be more narrow as  $R$  increases.

### 3.3. Effect of PAL addition on the oxygen quenching of pyrene and pyrene derivatives incorporated to DODAC liposomes

The dynamics of fluorescence quenching of pyrene and pyrene derivatives has been widely employed to characterize liposome bilayers [34,35]. The most relevant intra-vesicle properties invoked to account for rates of fluorescence quenching of probes incorporated in liposome bilayer are the oxygen concentration and the oxygen mobility. The experiments discussed earlier, indicate that PAL incorporation in DODAC liposomes at lower  $R_e$  does not produce significant changes in microviscosity of “core” bilayer but the main effect is to prevent the water entrance to the liposome. In consequence, it can be expected that quenching rate constants of pyrene and/or pyrene derivatives by oxygen inside the liposome, increases as the PAL content increases. The lipidic volume in DODAC LUVs is enough to guarantee that probe–oxygen interaction rates will be then determined only by the intra-vesicle properties, and will be almost completely independent of the properties of the surrounding solvent. The apparent rate constants for quenching of

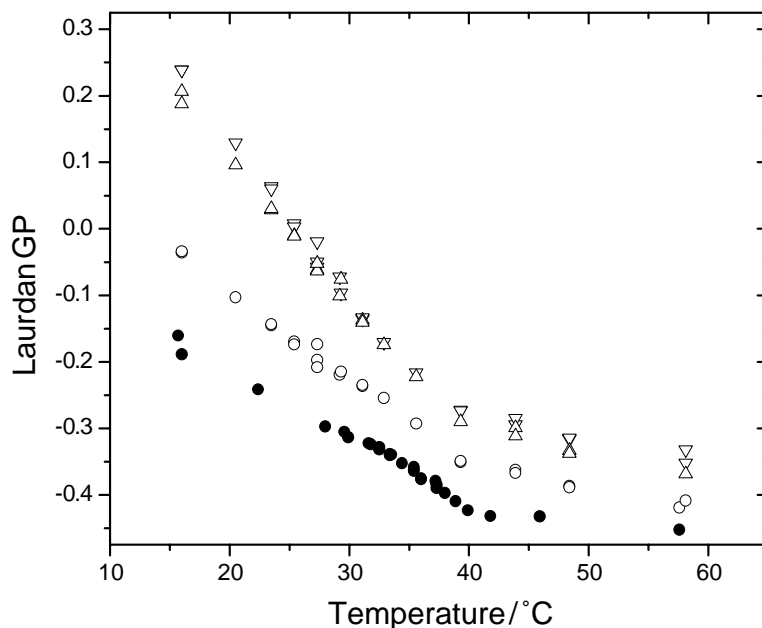


Fig. 7. Dependence of Laurdan GP upon temperature in DODAC–PAL liposomes. [LAU] = 6  $\mu$ M. [PAL]/[DODAC] ratio ( $R$ ): (●) 0; (○) 0.7; (▽) 1.3; (△) 1.9.

pyrene and pyrene derivatives by oxygen ( $k_{ox}$ ) in DODAC and DODAC/PAL liposomes, were determined from Stern–Volmer plots, by measuring the probe lifetime in nitrogen saturated, air saturated and oxygen saturated solutions. Table 1 shows the results obtained that are similar to those reported by Abuin and Lissi for pure DODAC LUVs [34].

The observed values for  $k_{ox}$  in DODAC liposomes, increase upon PAL incorporation, for  $R$  values below  $R_e$ . The increase of  $k_{ox}$  on PAL addition can be explained in terms of release of water molecules from

Table 1

Values of  $k_{ox}$  for the quenching of pyrene and pyrene decanoic acid in DODAC and PAL/DODAC vesicles at 25 °C

Derivative	[PAL]/[DODAC]	$k_{ox}$ ( $\times 10^6$ s $^{-1}$ )
Pyrene	0.00	4.01 $\pm$ 0.11
Pyrene	0.40	6.43 $\pm$ 0.12
Pyrene	0.84	6.41 $\pm$ 0.14
Pyrene	1.56	6.65 $\pm$ 0.03
PyC10	0.00	3.41 $\pm$ 0.10
PyC10	0.44	4.20 $\pm$ 0.11
PyC10	1.00	5.04 $\pm$ 0.14

the region in which pyrene is located (near to the interface according to the I/III ratio at 25 °C). The decrease of microenvironment polarity due to PAL addition, increase of oxygen solubility and  $k_{ox}$  augment, although PAL addition can drive the probe to move deeper inside the bilayer, where oxygen concentration is higher, effect that cannot be disregarded a priori. Additional data supporting the increase of oxygen solubility upon PAL addition were obtained by measuring the apparent quenching rate constant of an anchored probe in the same conditions. The values of  $k_{ox}$  obtained employing PyC10, that is fixed to the bilayer by interaction between the terminal carboxylic group and the cationic head group of DODAC, increases with PAL incorporation in the liposome bilayer as shown in Table 1. Taking into account that microviscosity does not undergo significant changes due to PAL incorporation (as was sensed by DPH at the same  $R$  range), and that both the oxygen diffusion coefficient and the  $k_q$  values inside the bilayer must remain almost constant, we can conclude that oxygen solubility in the lipidic phase increases as a consequence of water entrance blockage.

#### 4. Conclusions

PAL addition into DODAC liposomes induces structural changes in the liposome bilayer before the ‘solubilization’ process takes place. Light dispersion data indicate a liposome size increase, an unusual behavior for LUVs. The superficial sucrose moiety acts as a physical barrier that restricts access of water molecules to the bilayer, probably also forcing water structuring in the interface. These changes in the surface are also reflected in the inner bilayer as changes of polarity and fluidity of the probe surroundings (pyrene and Laurdan), but apparently deeper microenvironments are not affected.

#### Acknowledgements

This work was funded by I-12-2/2001, DID from University of Chile.

#### References

- [1] N. Deo, P. Somasundaran, *Colloids Surf. A* 186 (2001) 33.
- [2] U. Kragh-Hansen, M. le Maire, J.V. Moller, *Biophys. J.* 75 (1998) 2932.
- [3] A. de la Maza, J.L. Parra, *J. Am. Oil Chem. Soc.* 70 (1993) 699.
- [4] M. Ohnishi, H. Sagitani, *J. Am. Oil Chem. Soc.* 70 (1993) 679.
- [5] M.L. Jackson, C.F. Schmidt, D. Lichtenberg, B.J. Litman, A.D. Albert, *Biochemistry* 21 (1982) 4576.
- [6] D. Lichtenberg, *Biochim. Biophys. Acta* 821 (1985) 470.
- [7] F. Nomura, M. Nagata, T. Inaba, H. Hiramatsu, H. Otani, K. Takiguchi, *Proc. Natl. Acad. Sci.* 98 (2001) 2340.
- [8] T. Lian, R.J.Y. Ho, *J. Pharm. Sci.* 90 (2001) 667.
- [9] A. Lavi, H. Weitman, R.T. Holmes, K.M. Smith, B. Ehrenberg, *Biophys. J.* 82 (2002) 2101.
- [10] S. Kawakami, C. Munakata, S. Fumoto, F. Yamashita, M. Hakida, *J. Pharm. Sci.* 90 (2001) 105.
- [11] C.S. Jayaraman, *J. Pharm. Sci.* 85 (1996) 1082.
- [12] H.E. Junginger, *Cosmetics Toiletries* 106 (1991) 45.
- [13] M.F. Francis, G. Dhara, F.M. Winnik, J.C. Leroux, *Biomacromolecules* 2 (2001) 741.
- [14] S. Bhattacharya, S.N. Ghanashyam Acharya, *Langmuir* 16 (2000) 87.
- [15] R.K. Gupta, K. James, F.J. Smith, *J. Am. Oil Chem. Soc.* 60 (1983) 1908.
- [16] A. Ducret, A. Giroux, M. Trani, R. Lortie, *J. Am. Oil Chem. Soc.* 73 (1996) 109.
- [17] H. Mollee, J. De Vrind, T. De Vringer, *J. Pharm. Sci.* 89 (2000) 930.
- [18] C.-O. Rentel, J.A. Bouwstra, B. Naisbett, H.E. Junginger, *Int. J. Pharm.* 186 (1999) 161.
- [19] J.C.-M. Lee, R.J. Law, D.E. Discher, *Langmuir* 17 (2001) 3592.
- [20] M. Viard, J. Gallay, M. Vincent, M. Paternostre, *Biophys. J.* 80 (2001) 34.
- [21] F.M. Harris, K.B. Best, J.D. Bell, *Biochim. Biophys. Acta* 1565 (2002) 123.
- [22] T. Parasassi, G. De Stasio, G. Racagnan, R.M. Rusch, E. Gratton, *Biophys. J.* 60 (1991) 179.
- [23] T. Parasassi, E. Krasnowska, L. Bagatolli, E. Gratton, *J. Fluoresc.* 8 (1998) 365.
- [24] I.R. Vlahov, P.I. Vlahova, R.J. Lindhart, *J. Carbohydr. Chem.* 16 (1997) 1.
- [25] M.V. Encinas, E. Lemp, E.A. Lissi, *J. Photochem. Photobiol. B* 3 (1989) 113.
- [26] T. Inoue, in: M. Rossof (Ed.), *Vesicles*, vol. 62, Marcel Dekker, New York, 1996, p. 151.
- [27] D.C. Dong, M.A. Winnik, *Can. J. Chem.* 62 (1984) 2560.
- [28] G. Duportail, P. Lianos, in: M. Rossof (Ed.), *Vesicles*, vol. 62, Marcel Dekker, New York, 1996, p. 295.
- [29] E. Bruckner, P. Sonntag, H. Rehage, *Langmuir* 172 (2001) 308.
- [30] K. Kalyanasundaram, *Photochemistry in Microheterogeneous Systems*, Academic Press, Orlando, 1987, p. 41.
- [31] E. Lissi, A. Dattoli, E. Abuin, *Bol. Soc. Chil. Quim.* 30 (1985) 37.
- [32] Y. Liu, E.C.Y. Yan, K.B. Eisenthal, *Biophys. J.* 80 (2001) 1004.
- [33] E.A. Lissi, A. Abuin, M. Saez, A.L. Zanocco, A. Disalvo, *Langmuir* 8 (1992) 348.
- [34] E.B. Abuin, E.A. Lissi, *Prog. React. Kinet.* 16 (1991) 1.
- [35] Y. Barenholz, T. Cohen, R. Korenstein, M. Ottolenghi, *Biophys. J.* 60 (1991) 110.